Short communication

High sintering ability and electrical conductivity of Zn doped La(Ca)CrO$_3$ based interconnect ceramics for SOFCs

Mingfei Liu, Ling zhao, Dehua Dong, Songlin Wang,
Juan Diwu, Xingqin Liu, Guangyao Meng *

*USTC Laboratory for Solid State Chemistry & Inorganic Membranes, Department of Materials Science and Engineering,
University of Science and Technology of China (USTC), Hefei, 230026, PR China*

Abstract

In order to improve the sintering ability of La$_{0.7}$Ca$_{0.3}$CrO$_{3-\delta}$ (LCC), which has been considered as the interconnect material for SOFC but needs rather high temperature to densification, the ceramic powder with a nominal composition of La$_{0.7}$Ca$_{0.3}$Cr$_{0.95}$Zn$_{0.05}$O$_{3-\delta}$ (LCCZ) was prepared by auto-ignition process. The result was quite positive, that the specimens made by pressing the powder under 360 MPa and sintered at 1200 °C in air for 5 h showed a relative density of 95.2%. The electrical conductivity of LCCZ sintered at 1400 °C for 5 h reached 47.5 S cm^{-1} in air and 6.15 S cm^{-1} in hydrogen at 800 °C, which were much higher than the values of LCC. The thermal expansion coefficient of LCCZ was 11.5×10^{-6} K^{-1}, which well matches other components of SOFC.
© 2007 Elsevier B.V. All rights reserved.

Keywords: Interconnect ceramics; Doped lanthanum chromite; Sintering ability; Conductivity; SOFC

1. Introduction

Solid oxide fuel cell (SOFC) attracts more and more attention for its high efficiency and low pollution [1,2]. Interconnects, physically separating and electrically connecting the anode of one cell to the cathode of the next one, were one of the important components of SOFC stacks. Lanthanum chromite (LaCrO$_3$) based perovskite materials have been extensively investigated as interconnects for high temperature SOFCs due to its high thermal and chemical stability in both reducing and oxidizing atmosphere as well as good electrical conductivity [3,4]. However, its poor sintering ability and degradation of electrical conductivity at reduced temperatures have led to high fabrication cost and limited their applications at intermediate temperatures.

In order to improve the performance and durability while reducing the manufacturing cost of SOFCs, interconnect materials with high electrical conductivity and good sintering ability are required. Recently, a plenty of research on LaCrO$_3$ based perovskite materials has been done. Among the alkaline-earth doped LaCrO$_3$, the materials doped with Ca or Sr show a higher electrical conductivities. However, the sintering ability is still poor due to the vaporization of the chromium species during sintering [3,5]. In order to improve the sintering ability, lanthanum chromite doping with Cu, Co, Ni, V at B-site has been studied [6–8], but little attention has been paid to Zn.

In this work, the ceramic powder with a nominal composition of La$_{0.7}$Ca$_{0.3}$Cr$_{0.95}$Zn$_{0.05}$O$_{3-\delta}$ (LCCZ) was prepared by auto-ignition process. The sintering ability and electrical conductivity of LCCZ were investigated.

2. Experimental

2.1. Preparation of LCCZ powders

The LCCZ powder was synthesized by auto-ignition process. Stoichiometric amount of La(NO$_3$)$_3$, Ca(NO$_3$)$_2$, Cr(NO$_3$)$_3$ and Ca(NO$_3$)$_2$ was dissolved in deionized water. Citric acid as complexation/polymerization agent was then added with the ratio of citric acid/metal mole of 2:1. The solution was kept on a hotplate at 100 °C and stirred until a dark green gel formed. The gelled LCCZ-contained sample was baked in a drying cabinet at 120 °C overnight. Finally, the samples were calcined

* Corresponding author. Tel.: +86 551 3603234; fax: +86 551 3607627.
E-mail addresses: mgym@ustc.edu.cn, mfliu@mail.ustc.edu.cn (G. Meng).

at various temperatures, viz. 700, 800, 900, 1000, 1100 and 1200 °C, respectively for 2 h.

The structure of the LCCZ powers, which were calcined at various temperatures, was identified by X-ray diffraction (XRD) analysis on Philips PW 1730 diffractometer using Cu Kα radiation. The specific surface areas of the resulted powders were measured with the BET analyzer.

2.2. Measurements of electrical conductivity and thermal expansion coefficients

The powders were ball milled for 24 h using ethanol as medium and dried. Rectangular bar specimens were prepared by uniaxially pressing at 360 MPa and sintered in air at various temperatures, 1150, 1200, 1250, 1300, 1350 and 1400 °C, respectively for 5 h. The relative densities were determined by Archimedes' method. Electrical conductivity was studied using the standard dc four-probe technique on H.P. multimeter (Model 34401) from 500 to 800 °C. The thermal expansion behavior was examined on a dilatometer, SHIMADZU50, under the temperature ranging from 20 to 1000 °C at a heating rate of 10 °C min^{-1}. The morphological aspects of fractured surface of the specimens sintered at different temperatures were observed using scanning electron microscopy (SEM, model KYKY 1010).

3. Results and discussion

3.1. Powder characterization

Fig. 1 shows the XRD patterns of the LCCZ powders calcined at various temperatures. According to Fig. 1, major phase of doped LaCrO$_3$ has formed at 700 °C, and some intermediate compounds such as La$_2$CrO$_6$ still exist at that temperature. This powder when calcined at 800 °C shows mostly perovskite phase in association with a small amount of CaCrO$_4$. As the temperature increased from 800 to 900 °C, the phase of CaCrO$_4$ in the specimen has reached highest amount. It may, however, be noted that the peaks of CaCrO$_4$ shrunk with further increas-
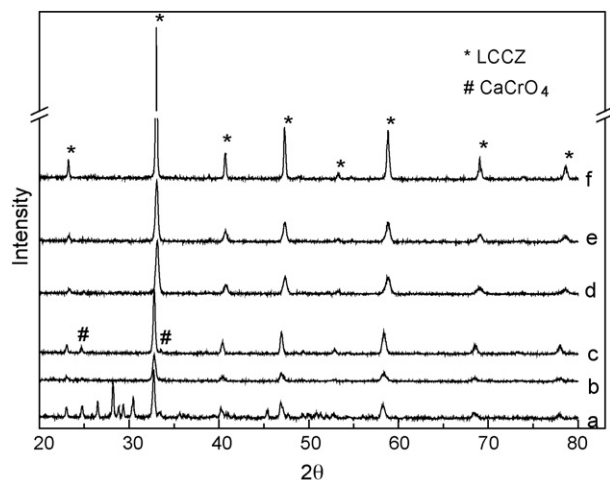

Fig. 1. XRD patterns of LCCZ powder calcined in air at various temperatures for 2 h. (a) 700 °C; (b) 800 °C; (c) 900 °C; (d) 1000 °C; (e) 1100 °C; (f) 1200 °C.

ing the temperature from 900 to 1200 °C, and disappeared at 1200 °C eventually. At the same time, the peak of the perovskite shift to larger angle (32.8–33.04). The shift may be reasonably explained by the contraction of lattice as Ca dissolving into the structure. Chakraborty et al. [9] and Sakai et al. [10] reported that presence of the minor phase of CaCrO$_4$ would create liquid phase sintering to benefit the densification. As mentioned above that the sample calcined at 900 °C forms the highest amount of CaCrO$_4$, thus we pre-heated the powder samples at 900 °C.

The BET specific surface area of LCCZ powder calcined at 900 °C, was 3.437 m^2 g^{-1} and the average particle size was about 1.05 μm with a narrow particle size distribution. The sintering shrinkage of the pellets made from this powder was 21.7% at 1400 °C.

3.2. The sintering behavior

Fig. 2(a) shows the relative density of LCCZ sintered in air at various temperatures for 5 h. As we can see, the relative density of LCCZ increases sharply from 84% for the sample fired at 1150 °C to 95.2% for that sample obtained at 1200 °C. Further increasing the sintering temperature up to 1400 °C, the relative density gradually increases to 98.7%. Many investigators reported that the pure La$_{0.7}$Ca$_{0.3}$CrO$_3$(LCC) sintered at a high temperature associated with a marked decrease on the relative density, which was attributed to the appreciable volatilization loss of chromium oxide in oxidizing atmosphere [9,11]. In LCCZ system, the partial substitution of Zn at Cr-site restrained the volatilization of chromium. Sakai et al. [10] reported that the Cr deficiency (y) in La$_{1-x}$Ca$_x$Cr$_{1-y}$O$_3$ could promote the sintering process at a lower temperature. In our work, no Cr deficiency was designed in LCCZ. However, Zn at Cr-site would form Zn–O valence and reduce the concentration of Cr–O in the Cr(Zn)O$_6$ structure, which likely behaved with the similar effect. As a comparison the specimen of pure LCC synthesized using the same method only achieved a relative density of 78.8% when sintered at 1400 °C for 5 h. This demonstrates that Zn doped at Cr-site significantly promotes the sintering process of LCC-based materials.

The sintering ability of the powders calcined at 800, 900, 1000, 1100 and 1200 °C, respectively, were also investigated in the present work. The Rectangular bar specimens were finally sintered at 1250 °C for 5 h. The effects of the calcining temperatures on the relative density of LCCZ are shown in Fig. 2(b). It is clear that among the all samples the powder calcined at 900 °C achieved the highest relative density (96.4%). With the calcined temperatures increasing to 1200 °C, the relative density decreases gradually from 96.4 to 94.7%. This result is consistent with the amount of CaCrO$_4$ phase in the powders for various calcining temperatures (in Fig. 1). This might be an evidence that existence of CaCrO$_4$ is able to enhance the sintering process. Of course, the bigger particle size of the powders formed at higher temperature may be another reason for the sintering activity. However, it should be pointed out that the LCCZ powder even being calcined at 1200 °C for 2 h still achieved a relative density of 94.7% at 1250 °C. This illustrates that the excellent sintering
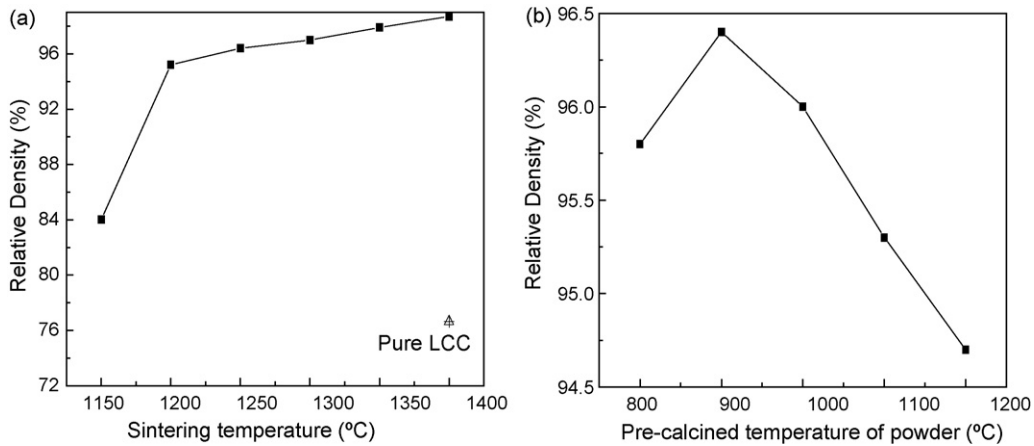
Fig. 2. (a) Effect of sintering temperatures on densification of LCCZ; (b) effect of calcined temperatures on densification of LCCZ.

ability of LCCZ should be attributed to the effect of Zn as a dopant.

Fig. 3 presents the SEM pictures of the fractured surface of LCCZ sintered at various temperatures. It can be seen that the specimen sintered at 1200 °C for 5 h is already quite dense and only a few isolated pores are visible at the grain boundary. As increasing the sintering temperature, the grain size develops bigger with more perfection. The average grain size is about 2–3 μm for the specimen sintered at 1200 °C and 4–5 μm for 1400 °C.

3.3. Electrical conductivity of LCCZ

Fig. 4(a) shows the temperature dependences of the electrical conductivity of LCCZ in air at various temperatures. The electrical conductivity sharply increases from 33.2 to 45.7 S cm^{-1} at 800 °C in air when the sintering temperature increased from 1150 to 1200 °C. While the sintering temperature increased from 1200 to 1400 °C, the conductivity gradually increases to 47.5 S cm^{-1}, which is 2.13 times higher than that of pure LCC (22.3 S cm^{-1} at 800 °C). The increase in the electrical conductivity certainly is related to the higher density of LCCZ than LCC, but it might also have some other factors. It is worthy to note that even at 500 °C, the conductivity of LCCZ sintered above 1200 °C is higher than 34.5 S cm^{-1}.

The linear behavior of ln σT versus $1/T$ plots (Fig. 4(a)) shows the convincing evidence that thermally activated hopping of small polarons is responsible for the conduction process. The relationship between the electrical conductivity σ and temperature T, can be described as follows,

$$\sigma = \frac{A}{T} \exp\left(-\frac{E_a}{RT}\right) \tag{1}$$

where σ is the electrical conductivity, A is a pre-exponent constant, T is the absolute temperature, R is gas constant and E_a is the activation energy of conduction. The activation energy calculated for LCCZ is about 13–14.5 kJ mol^{-1}, which is a little lower than pure LCC (16.5 kJ mol^{-1}), indicating the improved

conduction path in LCCZ resulted by Zn substitution to Cr sites.

As presented in Fig. 4(b), the calcined temperatures of the powders also remarkably effect on the electrical conductivity of the sintered specimens. The conductivity of the sample calcined 900 °C shows the highest values at different testing temperatures. The variation regularity agrees well with the relative density of the samples (see Fig. 2(b)), higher density shows higher electrical conductivity.

Fig. 4(c) illustrates the temperature dependence of the electrical conductivity of LCCZ (sintered at 1400/5 h) in H$_2$. A fairly high conductivity of 2.06 S cm^{-1} at 500 °C and 6.15 S cm^{-1} at 800 °C are achieved, which are much higher than the values of 0.45 and 3.01 S cm^{-1} for pure LCC at corresponding temperatures. 1 S cm^{-1} is the minimum acceptable electrical conductivity for the application of interconnects in SOFC community [12]. Larger conductivity of LCCZ will further decrease the ohmic loss in SOFCs stacks caused by interconnect material. Thus, LCCZ should be an appropriate choice for SOFC operating at intermediate temperatures (<800 °C). The Ea value of LCCZ is about 27–38 kJ mol^{-1}, which is much lower than that of pure LCC (50.7 kJ mol^{-1}).

Doped LaCrO$_3$ has been recognized as a p-type conductor [13,14]. The predominant defect species in LCCZ can be assumed to be Ca$'_{La}$, Zn$'_{Cr}$, Cr$_{Cr}^{\bullet}$ (Cr$_{Cr}^{\bullet}$ is Cr^{4+} on Cr-site, the same implication with electron hole) and $V_O^{\bullet\bullet}$, using the Kroger–Vink notation. The electronic charge carriers are considered to be localized at the Cr-sites and the electrical conduction is mainly performed by a so-called small-polaron hopping mechanism. The negatively charged Ca$'_{La}$ and Zn$'_{Cr}$ are compensated by the valence change of chromium ions from Cr^{3+} to Cr^{4+} (thus enhanced the electrical conduction) and the formation of oxygen vacancies (ionic compensation mechanism [15]), The neutrality condition is simply descried as:

$$[Ca'_{La}] + [Zn'_{Cr}] = [Cr_{Cr}^{\bullet}] + 2[V_O^{\bullet\bullet}] \tag{2}$$

where [ ] indicates concentration. The oxygen vacancy concentration is a function of P_{O_2} and temperature. With decreasing
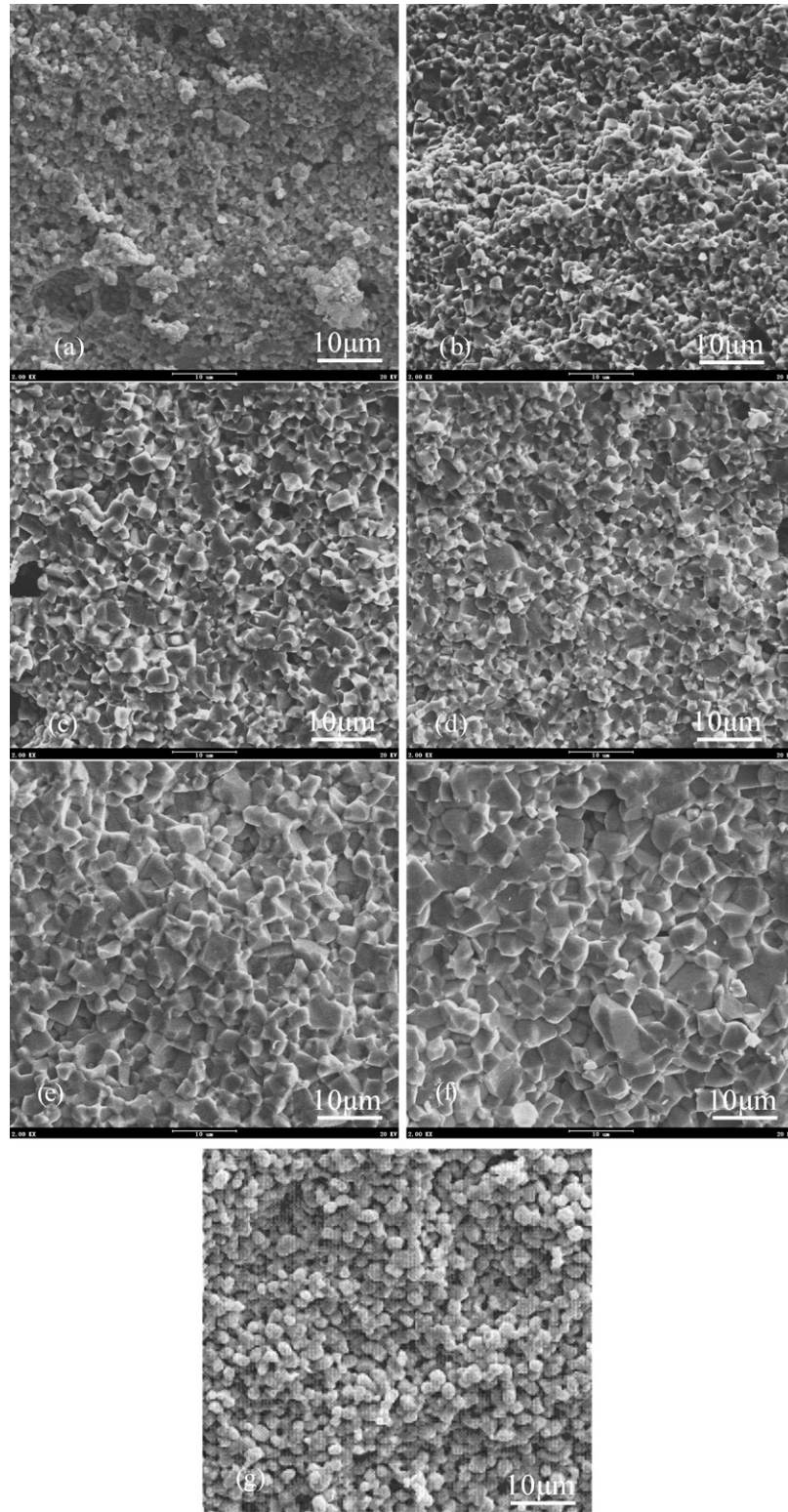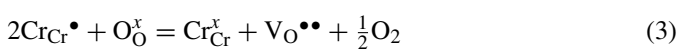
Fig. 3. Fractured surface of micrograph of LCCZ sintered for 5 h at, (a) 1150 °C; (b) 1200 °C; (c) 1250 °C; (d) 1300 °C; (e) 1350 °C; (f) 1400 °C; (g) pure LCC sintered at 1400 °C for 5 h.

P_{O_2} (at constant T) and/or increasing the temperature (at constant P_{O_2}), the oxygen vacancies are formed at the expense of losing $Cr_{Cr}^\bullet$:

$$2Cr_{Cr}^\bullet + O_O^x = Cr_{Cr}^x + V_O^{\bullet\bullet} + \tfrac{1}{2}O_2 \qquad (3)$$

The electrical conductivity (σ) is determined by the concentration of charge carrier (electron hole) and its mobility (μ), as represented with
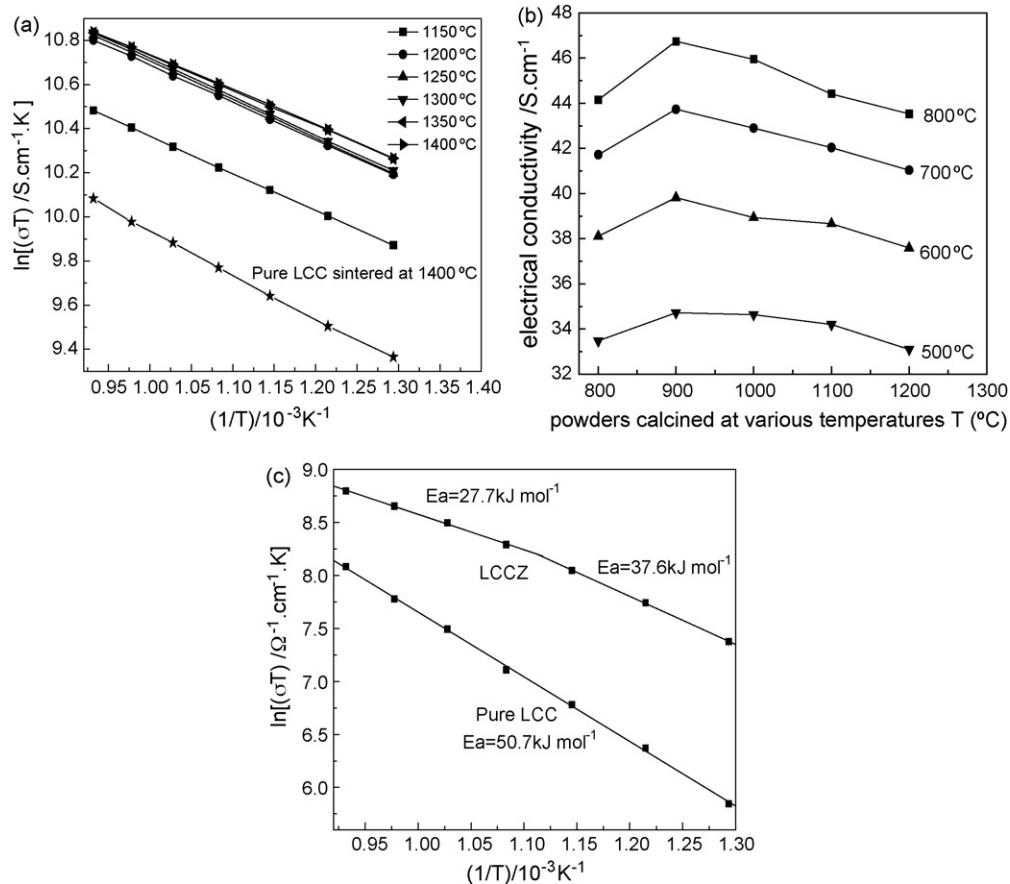
$$\sigma = [Cr_{Cr}^\bullet]\mu \qquad (4)$$

Fig. 4. (a) Electrical conductivity of LCCZ at various sintering temperatures in air; (b) effect of the calcining temperatures on the conductivity of the specimens in air at various temperatures; (c) electrical conductivity of LCCZ in H_2.

The mobility of charge carriers depends on temperature and their hoping energy [16]. In high oxygen pressure, the formation of oxygen vacancies is negligible and charge compensation in LCCZ takes place via the transition of Cr^{3+} to Cr^{4+}. Thus, Zn doped at Cr site increases the concentration of electron holes and hence the conductivity of LCCZ would be higher than that of pure LCC. Of course, the lower conductivity of LCC might also be resulted from the lower relative density (see Fig. 2(a)). And lattice structure adjusted by a larger ionic size of Zn ions at Cr-site would possibly modify the mobility and enhance the electrical conductivity in the former case, that can interpret the lower conduction activation energy and higher conductivity values obtained experimentally described above.

When the ambient from oxidizing changes into reducing atmosphere, the concentration of oxygen vacancies in the specimens is likely to increase associated with some Cr^{4+} reducing to Cr^{3+} according to Eq. (3), and the conductivity would significantly decrease. As mentioned previously, the electron holes are localized in the lattice of oxygen-octahedral (CrO_6) perovskite. The increase in ionic size due to reduction of Cr^{4+} into Cr^{3+} would enhance the Cr–O–Cr bond length, which would inhibit polaron transport and lead to a higher activation energy than that in air [17]. The activation energy of LCCZ is much lower than that of LCC, which may result from the adjustment of the oxygen-octahedral caused by the addition of Zn at Cr-site together with oxygen vacancy concentration expansion. It may,

however, be noted that a curvature is observed at about $650\,^\circ C$ for LCCZ in H_2 (Fig. 4(c)). A similar curvature has been observed in the materials with oxygen vacancies [18,19]. The curvature in LCCZ may attribute to the order–disorder transition of oxygen vacancy or the formation of dopant (Zn) cation-oxygen vacancy associates. For LCCZ, Zn doped at Cr site may act not only just as traps for isolated oxygen vacancies, but also as nucleating centers for the formation of ordered-vacancy clusters.

3.4. Thermal expansion measurements

SOFCs operate at high temperatures and should endure the thermal cycle from room temperature to operating temperature, therefore the thermal expansion coefficient (TEC) of interconnect must close to those of the other cell components to minimize the thermal stresses. The thermal expansion almost linearly increased with temperature. Further calculation indicated that the average TEC of LCCZ between 200 to $1000\,^\circ C$ is $11.5 \times 10^{-6}\,K^{-1}$, which was very much compatible with other cell components like YSZ electrolyte, Sr substituted lanthanum manganite cathode and Ni–YSZ anode used in SOFC.

4. Conclusion

The ceramic interconnect $La_{0.7}Ca_{0.3}Cr_{0.95}Zn_{0.05}O_{3-\delta}$, prepared by auto-ignition process showed high sintering ability.

M. Liu et al. / Journal of Power Sources 177 (2008) 451–456

95.2% relative density was achieved at a temperature as low as 1200 °C. The electrical conductivity of dense LCCZ was higher than 45.7 and 34.5 S cm^{-1} at 800 and 500 °C in air, respectively. 2.06–6.1 S cm^{-1} was got in H$_2$ in the temperature range of 500–800 °C. The thermal expansion coefficient of LCCZ was 11.5×10^{-6} K^{-1}, which was very close to that of other cell component. The high sintering ability, electrical conductivity and suitable TEC of the material indicated that it was suitable for being used as an interconnect material for SOFC.

Acknowledgements

References

[1] S.C. Singhal, Solid State Ionics 152–153 (2003) 405–410.
[2] N.Q. Minh, J. Am. Ceram. Soc. 76 (1993) 563–588.
[3] J.W. Fergus, Solid State Ionics 71 (2003) 1–15.
[4] S.C. Singhal, K. Kendall, High Temperature Solid Oxide Fuel Cells, Elsevier, Kidlington, 2003, p. 173.
[5] M. Mori, J. Electrochem. Soc. 149 (2002) A797.
[6] G.Y. Lee, R.H. Song, J.H. Kim, et al., J. Electroceram. 17 (2006) 723–727.
[7] R. Koc, H.U. Anderson, J. Mater. Sci. 9 (1992) 285.
[8] M. Moria, N.M. Sammes, Solid State Ionics 146 (2002) 301–312.
[9] A. Chakraborty, R.N. Basu, H.S. Maiti, Mater. Lett. 45 (2000) 162–166.
[10] N. Sakai, T. Kawada, H. Yokokawa, et al., J. Am. Ceram. Soc. 76 (1995) 609–616.
[11] L.P. Rivas-Vazquez, J.C. Rendon-Angeles, J.L. Rodriguez-Galiciaa, C.A. Gutierrez-Chavarria, K.J. Zhu, K. Yanagisawa, J. Eur. Ceram. Soc. 26 (2006) 81–88.
[12] N.Q. Minh, C.R. Horne, S. Liu, et al., Proceedings of the 25th Intersociety Energy Conversion Engineering Conference vol. 13, American Institute of Chemical Engineers, New York, 1990, p. 256.
[13] W.Z. Zhu, S.C. Deevi, Mater. Sci. Eng. A348 (2003) 227–243.
[14] A. Zuev, L. Singheiser, K. Hilpert, Solid State Ionics 147 (2002) 1–11.
[15] D.B. Meadowcroft, Br. J. Appl. Phys. 2 (1969) 1225.
[16] I. Yasuda, M. Hishinuma, Solid State Ionics 80 (1995) 141–150.
[17] S.W. Tao, J.T.S. Irvine, J. Electrochem. Soc. 151 (2004) A252.
[18] K.Q. Huang, M. Feng, J.B. Goodenough, J. Am. Ceram. Soc. 81 (1998) 357.
[19] B.C.H. Steele, Solid State Ionics 129 (2000) 95–110.